

Correlated quantum screening model for non-ideal plasmas

Fuyang Zhou,¹ Yizhi Qu,² Junwen Gao,³ Yulong Ma,¹ Yong Wu,^{1, a)} and Jianguo Wang¹

¹Key Laboratory of Computational Physics, Institute of Applied Physics and Computational Mathematics, Beijing, 100088, China

²School of Optoelectronics, University of Chinese Academy of Sciences, Beijing, 100049, China

³Laser Fusion Research Center, China Academy Of Engineering Physics, Mianyang, 621900, China

(Dated: 22 July 2020)

For an ion embedded in dense plasma, the electron screening will greatly alter its atomic properties and leads to the various phenomena, such as ionization potential depression (IPD) and line shift etc. An accurate description of electron screening effect is of crucial importance in the simulations of radiation transport and Equation of State in dense plasmas. In the present work, an electron screening model considering electron correlation and quantum degeneracy effects is proposed for treating non-ideal plasma. In this model, the Fermi-Dirac distribution is modified to include the electron correlation effect, and plasma electrons are assumed to be able to occupy the bound orbitals (with negative energy) of an embedded ion. When investigating the screening effect on a specific bound state of the embedded ion, the quantum degeneracy between negative-energy electrons and the studied bound state is considered and leads to a dependence of the plasma-electron distribution on the specific bound state. The model is applied to calculate line shifts of He-like ion embedded in non-ideal plasma and much better agreements with the latest two experimental results are achieved in comparison with other screening models' calculations. It can be a useful tool for calculating atomic/molecular structure and dynamics processes within dense plasmas, and has potential applications to the investigation involving dense plasma, such as astrophysics, initial confinement fusion, and the study of matter in extreme conditions.

Keywords: Electron screening model, Dense plasma, line shift, pressure ionization

Since dense plasma exists widely in all types of stars¹, the interior of giant planets² and inertial confinement fusion^{3,4}, the studies of its thermodynamic and transport properties attract much attention. Examples of recent experimental investigations include the X-ray free-electron laser excited plasmas⁵⁻⁷, inertial confinement fusion experiments^{8,9} and laboratory opacity measurements^{10,11}. For an ion embedded in dense plasma, electron screening, which is the damping of electric fields caused by the presence of mobile electrons in plasmas, can significantly shift ionic energy levels toward the continuum, resulting in ionization potential depression (IPD) and line shift. These atomic energy shifts result in a significant modification of ionization balance in the plasma. Therefore, understanding the influence of electron screening on atomic properties is important for interpreting spectra, modeling opacity and equation of state (EOS) in dense plasmas^{12,13}. In addition, the investigation of electron screening in dense plasma is also of great interest from a fundamental viewpoint, since it reflects the complex quantum many-body interactions in a statistic manner. How to explicitly treat the many-body interaction of non-ideal plasma is still an open question up to now.

The well-known Debye-Hückel screening model¹⁴ is valid only for non-degenerate and weakly coupled plasmas. Thereafter, the Thomas-Fermi screening and self-consistent field ion-sphere models have been used to study the electron screening effects in degenerate plasmas^{15,16}. For the convenience of application, analytic solutions, such as uniform electron gas model¹⁷, Ecker-Kröll (EK) model¹⁸, Stewart-Pyatt

(SP) model¹⁹, and analytic fits to ion-sphere potentials²⁰⁻²², are proposed and widely used to calculate the IPDs and line shifts in dense plasmas. Due to the complicated many-body interactions and quantum effects involved, these models are proposed with various approximations and are applicable to the plasmas with specific conditions. Their reliabilities are questionable in treating non-ideal dense plasma and must be verified by comparing with experimental observations. Since the significant advances in obtaining uniform, well-characterized and high-energy-density plasmas, it becomes possible to measure the ionic level shift of warm- and hot-dense plasmas^{5,23-25}. Recently, Stillman *et al.*²⁵ and Beiersdorfer *et al.*²⁶ present their line-shift measurements of Al¹¹⁺ and Cl¹⁵⁺ in hot-dense plasmas as sensitive benchmarks for screening models. However, inconsistent results are shown in comparison with the predictions of the Li and Rosmej's analytical model²¹, which is a fit of the self-consistent field ion-sphere model. Thereafter, by employing numerical self-consistent field ion-sphere models^{27,28}, line-shift model based on Stewart-Pyatt screening potential²⁹ and other analytical fits of ion-sphere models^{27,30,31}, the agreements between theoretical results and measured shifts of $1s3p - 1s^2$ transition of Cl¹⁵⁺²⁶ are achieved. However, the line-shift measurements $1s2p - 1s^2$ transition of Al¹¹⁺²⁵ remains unexplained up to present days, since the available results of these models^{27,30,32} are shown to considerably underestimate the measured shifts. Therefore, a more general screening model is expected to explain both line-shift measurements.

In this letter, a correlated quantum screening model for non-ideal plasma is proposed, in which the plasma-electron density is obtained by using a modified Fermi-Dirac distribution and the electron correlation effect can be addressed based on

^{a)}Correspondence email address: wu_yong@iapcm.ac.cn

classical molecular dynamics (CMD) simulations. It should be noted that in this model the electrons from plasma environment are allowed to occupy the bound orbital of an embedded ion, and this leads to a dependence of the plasma-electron density distribution on the ionic bound state. As an application of our model, we calculate the line shifts of both $\text{Al}^{11+}(1s2p - 1s^2)$ transition and $\text{Cl}^{15+}(1s3p - 1s^2)$ transition, and good agreements with the two experiments^{25,26} are achieved. The present screening model can be used to investigate atomic/molecular structure and dynamic properties in dense plasmas, and is helpful for fundamental understanding of quantum many-body interactions.

CMD simulations - CMD method, in which the multi-particle interactions between ions and electrons are taken into account exactly, has been extensively employed in simulating the dynamical evolution and coupling properties of ultracold neutral plasmas (UNPs)^{33–35}. In our previous work³⁶, the evolution dynamics of UNPs has been simulated by this method and are consistent with experiment. In this work, in order to address the electron correlation effect on screening in non-ideal plasma, CMD simulations of UNPs are performed to obtain the electron density distribution, which is the key factor determining the screening effects and can be used to check the reliability of existing plasma screening models. Here, UNP is selected as a prototype of non-ideal plasma, for which the quantum degeneracy effects are negligible. For a typical UNP, the De Broglie wavelength for an electron at 5K ($\lambda \approx 60\text{nm}$) compare to the Wigner-Seitz radius at density of $10^9/\text{cm}^3$ ($a_{WS} \approx 6200\text{nm}$).

In this work, we present CMD simulations of two-component UNPs with electron density of $10^9/\text{cm}^3$ and electron temperatures of 5 K and 11.5 K. In simulations, 1000 electrons and 1000 ions ($Z=1$) are included, and the periodic boundary condition is applied to maintain constant density. Since considering static screening approximation, the mobility of ions is neglected and the ions are fixed in the evolutions. Then the electron density distribution that changed by a given ion located in the center of box is calculated by

$$\delta\rho(r) = \rho(r) - \rho'(r), \quad (1)$$

where $\rho(r)$ and $\rho'(r)$ are the average electron densities obtained from two simulations of the UNP with and without this ion, respectively. The time step $\Delta t = 0.5\text{ps}$ and the total evolution time $t = 25000\text{ps}$ are employed for each simulation. In order to reduce the statistical error, these simulations are repeated 1000 times with different random initial positions and velocities of electrons.

In figure 1, the CMD results of electron density deviations $\delta\rho(r)$ are compared with those of Fermi-Dirac distribution and the linear Debye-Hückel model with $\rho_0 = 10^9/\text{cm}^3$; $T_e = 5.5\text{K}$, $\Gamma_e = 0.49$ and $T_e = 11.5\text{K}$, $\Gamma_e = 0.23$, respectively. Here, $\Gamma_e = e^2/(4\pi\epsilon_0 a_{WS} k_B T_e)$ is the electron Coulomb coupling parameter, and a plasma is called ideal one for $\Gamma_e \ll 1$. It should be noted that the Fermi-Dirac distribution gives same results with the Boltzmann distribution, since the quantum degeneracy effects are negligible in the present cases. In Debye-Hückel model, the electron density is given by $\rho(r) = \rho_0[1 + e\Phi(r)/(k_B T)]$, which is obtained by lineariz-

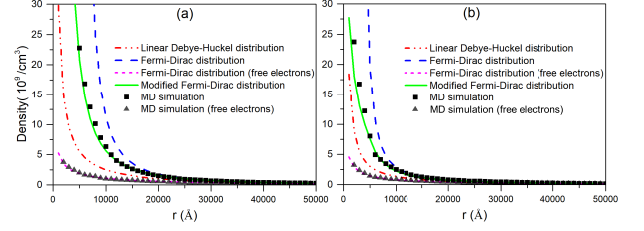


FIG. 1. The electron density fluctuation $\delta\rho(r)$ around an ion ($Z=1$, at origin) embedded in the UNPs with (a) $\rho_0 = 10^9/\text{cm}^3$, $T_e = 5.5\text{K}$ and (b) $\rho_0 = 10^9/\text{cm}^3$, $T_e = 11.5\text{K}$. The CMD simulated densities of electrons and free electrons are shown in **square** and **triangle**, respectively. Electron densities from Fermi-Dirac distribution (dash line), linear Debye-Hückel model (dash-dot line) and our modified Fermi-Dirac model (solid line) are shown to check their reliabilities. And the free-electron density from Fermi-Dirac distribution is shown in short dash line.

ing the Boltzmann distribution $\rho(r) = \rho_0 \exp[-e\Phi(r)/(k_B T)]$. But the electron densities obtained from MD simulations are significantly different with these from both Boltzmann distribution and Debye-Hückel model when $e\Phi(r)/(k_B T)$ is close or greater than 1, where the electron correlation effects have important influences on the plasma screening. The Boltzmann and Fermi-Dirac distributions work no more in such conditions, and will leads to the failure of popular Debye-Hückel and Thomas-Fermi screening model. Therefore, a more general screening model is required for treating the screening effects of non-ideal plasma, where the electron correlation effects become important.

Model formulation – In this work, the Fermi-Dirac distribution is modified to consider the electron correlation effect which is addressed based on the CMD results. The Fermi-Dirac statistics is derived based on the independent electron and mean-field approximations, and the number density of electrons is given as

$$\rho(r) = \frac{1}{2\pi^2\hbar^2} \int_0^\infty f_{FD}(p, \mathbf{r}) p^2 dp \quad (2)$$

$$\text{with } f_{FD}(p, \mathbf{r}) = \frac{1}{1 + \exp\left[\frac{1}{k_B T} \left(\frac{p^2}{2m_e} - e\Phi(\mathbf{r}) - \mu\right)\right]}, \quad (3)$$

where $f_{FD}(p, \mathbf{r})$ is the Fermi-Dirac distribution function, μ is the chemical potential, $\Phi(\mathbf{r})$ is the total effective potential at position \mathbf{r} , and p is the magnitude of electron momentum.

For an ion embedded in plasma, the free electrons are defined by the condition of

$$p > p_0 = \sqrt{2m_e e\Phi(\mathbf{r})}, \quad (4)$$

which guarantees that the kinetic energy of the free electrons is larger than the absolute value of the potential energy.

For comparison, figure 1 also present the free-electron in Fermi-Dirac distribution, in which p_0 is obtained by using

Debye-Hückel potential $\Phi_{DH}(\mathbf{r})$. Obviously, the free-electron density distribution is not adequate for describing the electron screening effect in moderately coupled plasma. Moreover, the CMD results of electron density with limitation of $p \geq \sqrt{2m_e e \Phi_{DH}(\mathbf{r})}$ are also presented in figure 1 and it agrees well with the one in Fermi-Dirac distribution. As learned in CMD simulations, the plasma electron can occupy the bound orbitals of the embedded ion, i.e. with momentum of $p < p_0$, due to the electron correlation effects. Throughout this article, the plasma electron with $p < p_0$ is called negative-energy electron to distinguish it from free electron and the studied bound state of embedded ion. The above comparisons indicate that the electron density discrepancies between CMD and other results mainly come from the different treatment of negative-energy electron distributions. Therefore, the Fermi-Dirac distribution can be modified reasonably to obtain consistent electron density distribution, in which the electron correlations are well considered.

In the present CMD simulations, there is one implicit assumption that the negative-energy electrons are evolve from free electrons through collisions. For the negative-energy electron with $p < p_0$, the energy of the correlated collided electron should be restricted to be larger than $\varepsilon_r = (p^2 - p_0^2)/2m_e$. Therefore, such an energy restriction of collided electron should be applied to describe the electron-electron correlation effect and modify the distribution function of negative-energy electrons as

$$f_{FD}(p, \mathbf{r}, \mathbf{r}') = f_{FD}(p, \mathbf{r}) \frac{\int_{\sqrt{\varepsilon_r/2m_e}}^{\infty} f_{FD}(p', \mathbf{r}') p'^2 dp'}{\int_0^{\infty} f_{FD}(p', \mathbf{r}') p'^2 dp'}, \quad (5)$$

which is depends on the position of the collision (i.e. \mathbf{r}'). In this letter, in order to illustrate the main influence of electron correlation on negative-energy electron distribution and obtain an analytic expression, Boltzmann distribution function is employed instead of $f_{FD}(p', \mathbf{r}')$ in the correction term, and then the distribution function is given by

$$f_{FD}(p, \mathbf{r}, \mathbf{r}') = f_{FD}(p, \mathbf{r}) \frac{\int_{\sqrt{\varepsilon_r/2m_e}}^{\infty} \frac{\exp\left(-\frac{p'^2}{2m_e k_B T}\right) p'^2 dp'}{\int_0^{\infty} \exp\left(-\frac{p'^2}{2m_e k_B T}\right) p'^2 dp'} , \quad (6)$$

$$= f_{FD}(p, \mathbf{r}) \left(2\sqrt{\frac{\varepsilon_r}{\pi k_B T}} \exp\left(\frac{\varepsilon_r}{k_B T}\right) + \text{Erfc}\left(\sqrt{\frac{\varepsilon_r}{k_B T}}\right) \right)$$

where $\text{Erfc}(x)$ is the error function. For the UNP and hot-dense plasmas studied here, this simplification is reasonable since the condition of $-\mu/k_B T \gg 1$ (weak degeneracy) is satisfied. Using this new distribution function, electron density $\rho(\mathbf{r})$ is obtained by

$$\rho(\mathbf{r}) = \frac{1}{2\pi^2 \hbar^2} \left(\int_0^{p_0} f(p, \mathbf{r}) p^2 dp + \int_{p_0}^{\infty} f_{FD}(p, \mathbf{r}) p^2 dp \right) \quad (7)$$

where the effective potential $\Phi(\mathbf{r})$ is dependent on $\rho(\mathbf{r})$ and can be calculated though a self-consistent iteration process.

In this model, the negative-energy electron distribution is modified by considering electron correlation effect, and will

significantly change the total electron distribution and screening effect of non-ideal plasmas. For classical UNP, its reliability can be validated straightforwardly by CMD simulations. As shown in figure 1, using the modified Fermi-Dirac distribution, good agreements are obtained in comparison with the results of CMD simulations for $\Gamma_e = 0.49$ and 0.23. These agreements reveal that the electron-electron correlations are well considered in the modify distribution function.

Line-shift calculations – In order to further evaluate its validity, the line shifts investigated in the recent experiments of hot-dense plasmas^{25,26} are calculated. In the line-shift calculations, the effects of bound state of the ion should be taken into account. On the one hand, the degeneracy effect between bound electrons and negative-energy plasma electrons is considered in our model. For an incompletely ionized ion within ground state, the energy of a plasma electron ε_p cannot be lower than the energy of outermost bound electron ε_b since the lower-energy orbitals are occupied. Therefore, the limitation $\varepsilon_p > \varepsilon_b$ is applied on the distribution of plasma electrons. Despite excited initial states involved in the calculation of line shifts, ε_b will always be the orbital energy of outermost bound electron not only because of the quantum degeneracy but also due to the condition of experiments. It will be discussed later in the comparison of line-shift calculations with experiments. On the other hand, the distribution of bound electrons will influence the total effective potential $\Phi(\mathbf{r})$. For a given ion located at origin, $\Phi(\mathbf{r})$ is given by

$$\Phi(\mathbf{r}) = \int \frac{e}{4\pi\varepsilon_0 |\mathbf{r} - \mathbf{r}'|} [Z\delta(\mathbf{r}') - \rho_b(\mathbf{r}') - \delta\rho(\mathbf{r}')] d\mathbf{r}', \quad (8)$$

where $\delta\rho(\mathbf{r}) = \rho(\mathbf{r}) - \rho_0$ is the plasma-electron density fluctuation induced by the ion, and the density of bound electrons $\rho_b(\mathbf{r})$ is calculated by

$$\Phi(\mathbf{r}) = \int \frac{e}{4\pi\varepsilon_0 |\mathbf{r} - \mathbf{r}'|} [Z\delta(\mathbf{r}') - \rho_b(\mathbf{r}') - \delta\rho(\mathbf{r}')] d\mathbf{r}'. \quad (9)$$

Here q_j is the occupation number of electrons in the orbital j , and $P_j(r)$ and $Q_j(r)$ are the relativistic radial wave functions of the large and small components, respectively. The bound wave functions are obtained by using multi-configuration Dirac-Fock approach^{37,38}.

Once the plasma-electron densities have been determined, the level shift for orbital j can be given by

$$\Delta\varepsilon_j = \int_0^{\infty} [P_j^2(r) + Q_j^2(r)] V(r) r^2 dr \quad (10)$$

$$\text{with } V(r) = \int \frac{e^2}{4\pi\varepsilon_0 |\mathbf{r} - \mathbf{r}'|} \delta\rho(\mathbf{r}') d\mathbf{r}' ,$$

where $V(r)$ is the potential energy derived from plasma electrons.

In the line-shift experiments for $1s2p - 1s^2$ transition in Al^{11+} in plasmas with electron densities ρ_e of $1 - 5 \times 10^{23}/\text{cm}^3$ and temperatures T_e of 250-375 eV²⁵ and $1s3p - 1s^2$ transition in Cl^{15+} with ρ_e of $3 - 6 \times 10^{23}/\text{cm}^3$ and T_e of 600-650 eV²⁶, the Coulomb coupling parameters Γ_e are as low as about 0.05. However, it is found that the electron density distributions around highly charged ions embedded in these hot-dense plasmas cannot be described by

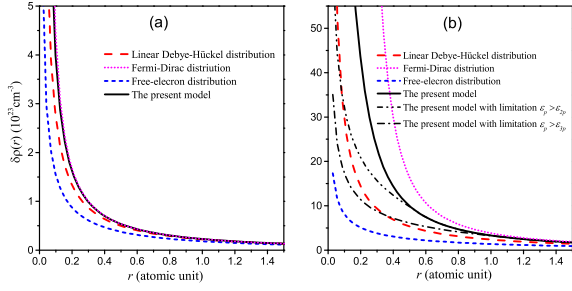


FIG. 2. Comparison of electron density deviation $\delta\rho(r)$ induced by an Al ion (at origin) for different models, for ion charge of (a) $Z=1$, (b) $Z=11$. The mean electron density ρ_0 is $3 \times 10^{23}/\text{cm}^3$, the temperature T_e is 300 eV, and the orbital energies of $2p$ and $3p$ are about -498 eV and -217 eV, respectively.

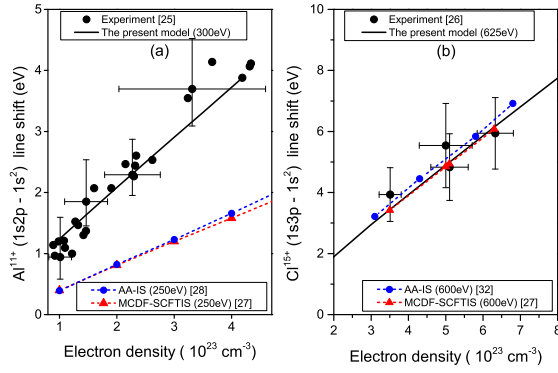


FIG. 3. Comparison of The the line shifts from experimental measurements^{25,26} and the present screening model, as well as numerical calculations of MCDF-SCFTIS²⁷ and AA-IS models^{28,32}. (a) $1s2p - 1s^2$ transition in Al^{11+} , (b) $1s3p - 1s^2$ transition in Cl^{15+} .

Debye-Hückel or Thomas-Fermi model. For example, different theoretical results of the electron deviation $\delta\rho(r)$ induced by a given Al ion in hot-dense plasma with $\rho_0 = 3 \times 10^{23}/\text{cm}^3$, $T_e = 300$ eV and $\Gamma_e = 0.052$ are presented in figure 2. Here, the screening length λ of Debye-Hückel and Thomas-Fermi models are 4.442 and 4.449 in atomic unit, respectively, thus the lines of $\delta\rho(r)$ from these two models will be coincided in figure 2. For the case of $Z=1$, different distributions agree with each other in such a weakly coupled plasma. The present model naturally reduces to Fermi-Dirac distribution and Thomas-Fermi screening model in the weak-coupling limit. However, for the case of $Z=11$ (i.e. Al^{11+}) the present modified Fermi-Dirac distribution gives a much larger electron density around the ion than the one of linear Debye-Hückel distribution. Despite the small coupling strength of $\Gamma_e = 0.052$, the electron density distribution around the highly charged ion shows to be a non-linear function of potential. The Debye-Hückel and Thomas-Fermi models will work no longer to describe the electron screening effect around a highly charged ion.

In figure 3, the line shifts of $\text{Al}^{11+}(1s2p - 1s^2)$ and

$\text{Cl}^{15+}(1s3p - 1s^2)$ transitions from the present screening model are compared with experimental values^{25,26}, as well as the numerical calculations of multi-configuration-Dirac-Fock self-consistent finite-temperature ion-sphere model (MCDF-SCFTIS)²⁷ and average-atom ion-sphere model (AA-IS)^{28,32}. The calculations are done at $T = 300$ eV for $1s2p - 1s^2$ transition and at $T = 625$ eV for $1s3p - 1s^2$ transition. Despite that the self-consistent field ion-sphere model has been thought to be reliable for dense plasmas, MCDF-SCFTIS and AA-IS models largely underestimate the measured shifts of $1s2p - 1s^2$ transition. In Li and Rosmej's work²⁷, an analytical b-potential approach, which is based on MCDF-SCFTIS model and uses an adjustable parameter b to characterize the plasma-electron density, is also presented. It matches the measurements of $1s2p - 1s^2$ transition with $b = 4$ and $1s3p - 1s^2$ transition with $b = 2$, respectively, but the discrepancy of parameter b (i.e. different plasma-electron density distributions) is unexplained in their work. By using the present screening model, the line shifts are calculated without any adjustable parameter and are in reasonable agreement with both experiments. This reveals that our model can well describe the plasma-electron density distributions in these cases.

In our screening model, the limitation $\epsilon_p > \epsilon_b$, in which the ϵ_b is the outermost bound orbital energy, is used to guarantee the quantum degeneracy between bound and negative-energy plasma electrons. For $1s3p - 1s^2$ transition in Cl^{15+} , the initial state is excited, and the plasma electron can turn to $2s$ or $2p$ orbital. But we do not take account of its contributions in line-shift calculations, because of that the energy of $1s2l'3p - 1s^22l'$ transitions is far away from $1s3p - 1s^2$ transition and have not been included in the experimental measurements. For example, the energy difference between $1s2l'3p - 1s^22l'$ transitions and $1s3p - 1s^2$ transition is about 50-60 eV and considerably greater than the experimental full width at half maximum (FWHM) of $1s3p - 1s^2$ line (about 20 eV)²⁶. Therefore, the line shift of $1s3p - 1s^2$ transition are calculated by using the outermost bound orbital energy ϵ_{3p} , and the limitation $\epsilon_p > \epsilon_{2p}$ is applied in line-shift calculations for $1s2p - 1s^2$ transition.

For a further study of the quantum degeneracy effect between bound and plasma electrons, the plasma electron density deviations $\delta\rho(r)$ with limitations of different bound orbital energy (ϵ_{2p} and ϵ_{3p}) of Al^{11+} ion are presented in figure 2(b). It is found that the electron density around ion with limiting energy ϵ_{2p} are significantly larger than that with limiting energy ϵ_{3p} , and will lead to a stronger screening effect in present model. This reveals that the plasma-electron density distribution and its screening effect are sensitively dependent on the limiting energy ϵ_b , which is decided by the studied bound state as discussed above. By considering this dependence, good agreements with the two line-shift experiments are achieved. In contrast, the previous self-consistent field ion-sphere models, which cannot reflect the sensitive dependence of electron screening on bound state, failed to agree with the experiments.

In conclusion, the correlated quantum screening model, which incorporates the quantum degeneracy and electron correlation effects, is proposed and successfully describes the re-

cent experimental line-shifts measurements in hot-dense plasmas. In this model, the electron correlation effect is included based on modified Fermi-Dirac distribution, and the plasma electron is allowed to occupy the bound orbitals (with negative energy) of an embedded ion. It is found that the plasma-electron density distribution is sensitively dependent on the bound state and will significantly influences the level shift. Based on our model, a unified framework for describing dense plasma screening effects on different ions and specific bound states is proposed. More high-precision experiments are expected for examining its validity. Besides atomic structure, the present model also provides the basis for calculating various dynamics processes in dense plasmas, such as photon-ionization, electron-ion collision, Auger decay, dielectronic recombination, and ion-ion collision. We expect its applications in plasma physics, atomic and molecular physics, high-energy-density physics, astrophysics, and fusion science.

ACKNOWLEDGEMENTS

This work was supported by the National Key Research and Development Program of China under Grants No. 2017YFA0402300 and No. 2017YFA0403200 and the National Natural Science Foundation of China (Grants No.11474032, No.11774344, No.11704040, No.11534011 and No.U1530261).

- ¹R. J. Tayler, *The stars: their structure and evolution* (Cambridge University Press, 1994).
- ²R. Helled, J. D. Anderson, M. Podolak, and G. Schubert, *The Astrophysical Journal* **726**, 15 (2010).
- ³J. D. Lindl, P. Amendt, R. L. Berger, S. G. Glendinning, S. H. Glenzer, S. W. Haan, R. L. Kauffman, O. L. Landen, and L. J. Suter, *Physics of plasmas* **11**, 339 (2004).
- ⁴S. Hu, B. Militzer, V. Goncharov, and S. Skupsky, *Physical review letters* **104**, 235003 (2010).
- ⁵S. Vinko, O. Ciricosta, B. Cho, K. Engelhorn, H.-K. Chung, C. Brown, T. Burian, J. Chalupský, R. Falcone, C. Graves, *et al.*, *Nature* **482**, 59 (2012).
- ⁶O. Ciricosta, S. Vinko, H.-K. Chung, B.-I. Cho, C. Brown, T. Burian, J. Chalupský, K. Engelhorn, R. Falcone, C. Graves, *et al.*, *Physical review letters* **109**, 065002 (2012).
- ⁷O. Ciricosta, S. Vinko, B. Barbrel, D. Rackstraw, T. Preston, T. Burian, J. Chalupský, B. I. Cho, H.-K. Chung, G. Dakovski, *et al.*, *Nature communications* **7**, 1 (2016).
- ⁸O. Hurricane, D. Callahan, D. Casey, P. Celliers, C. Cerjan, E. Dewald, T. Dittrich, T. Döppner, D. Hinkel, L. B. Hopkins, *et al.*, *Nature* **506**, 343 (2014).
- ⁹M. R. Gomez, S. A. Slutz, A. B. Sefkow, D. B. Sinars, K. D. Hahn, S. B. Hansen, E. C. Harding, P. F. Knapp, P. F. Schmit, C. A. Jennings, *et al.*, *Physical review letters* **113**, 155003 (2014).
- ¹⁰J. E. Bailey, T. Nagayama, G. P. Loisel, G. A. Rochau, C. Blancard, J. Colgan, P. Cossé, G. Faussurier, C. Fontes, F. Gilleron, *et al.*, *Nature* **517**, 56 (2015).
- ¹¹T. Nagayama, J. Bailey, G. Loisel, G. Dunham, G. Rochau, C. Blancard, J. Colgan, P. Cossé, G. Faussurier, C. Fontes, *et al.*, *Physical review letters* **122**, 235001 (2019).
- ¹²D. Salzmann, *Atomic physics in hot plasmas*, 97 (Oxford University Press on Demand, 1998).
- ¹³H. R. Griem, *Principles of plasma spectroscopy*, Vol. 2 (Cambridge University Press, 2005).
- ¹⁴P. Debye and E. Hückel, *Z. Phys* **24**, 185 (1923).
- ¹⁵S. Ichimaru, *Reviews of Modern Physics* **54**, 1017 (1982).
- ¹⁶G. Zérah, J. Clérouin, and E. Pollock, *Physical review letters* **69**, 446 (1992).
- ¹⁷B. Crowley, *Physical Review A* **41**, 2179 (1990).
- ¹⁸G. Ecker and W. Kröll, *The Physics of Fluids* **6**, 62 (1963).
- ¹⁹J. C. Stewart and K. D. Pyatt Jr, *The Astrophysical Journal* **144**, 1203 (1966).
- ²⁰F. Rosmej, K. Bennadji, and V. Lisitsa, *Physical Review A* **84**, 032512 (2011).
- ²¹X. Li and F. Rosmej, *EPL (Europhysics Letters)* **99**, 33001 (2012).
- ²²X. Li, F. Rosmej, V. Lisitsa, and V. Astapenko, *Physics of Plasmas* **26**, 033301 (2019).
- ²³D. Hoarty, P. Allan, S. James, C. Brown, L. Hobbs, M. Hill, J. Harris, J. Morton, M. Brookes, R. Shepherd, *et al.*, *Physical review letters* **110**, 265003 (2013).
- ²⁴L. Fletcher, A. Kritcher, A. Pak, T. Ma, T. Doepfner, C. Fortmann, L. Divol, O. S. Jones, O. Landen, and H. A. Scott, *Physical Review Letters* **112**, 145004.1 (2014).
- ²⁵C. Stillman, P. Nilson, S. Ivancic, I. Golovkin, C. Mileham, I. Begishev, and D. Froula, *Physical Review E* **95**, 063204 (2017).
- ²⁶P. Beiersdorfer, G. Brown, A. McKelvey, R. Shepherd, D. Hoarty, C. Brown, M. Hill, L. Hobbs, S. James, J. Morton, *et al.*, *Physical Review A* **100**, 012511 (2019).
- ²⁷X. Li and F. Rosmej, *Physics Letters A* **384**, 126478 (2020).
- ²⁸Z.-B. Chen, *Journal of Quantitative Spectroscopy and Radiative Transfer* **237**, 106615 (2019).
- ²⁹M. F. Gu and P. Beiersdorfer, *Phys. Rev. A* **101**, 032501 (2020).
- ³⁰C. A. Iglesias, *High Energy Density Physics* **30**, 41 (2019).
- ³¹A. Singh, D. Dawra, M. Dimri, A. K. Jha, R. K. Pandey, and M. Mohan, *Physics Letters A* **384**, 126369 (2020).
- ³²Z.-B. Chen and K. Wang, *Radiation Physics and Chemistry* **172**, 108816 (2020).
- ³³T. C. Killian, *Science* **316**, 705 (2007).
- ³⁴T. Pohl, T. Pattard, and J. Rost, *Physical review letters* **94**, 205003 (2005).
- ³⁵L. Guo, R. Lu, and S. Han, *Physical Review E* **81**, 046406 (2010).
- ³⁶J. Gao, Y. Wu, Z. Zhong, and J. Wang, *Physics of Plasmas* **23**, 123507 (2016).
- ³⁷P. Jönsson, X. He, C. F. Fischer, and I. Grant, *Computer Physics Communications* **177**, 597 (2007).
- ³⁸P. Jönsson, G. Gaigalas, J. Bieroń, C. F. Fischer, and I. Grant, *Computer Physics Communications* **184**, 2197 (2013).